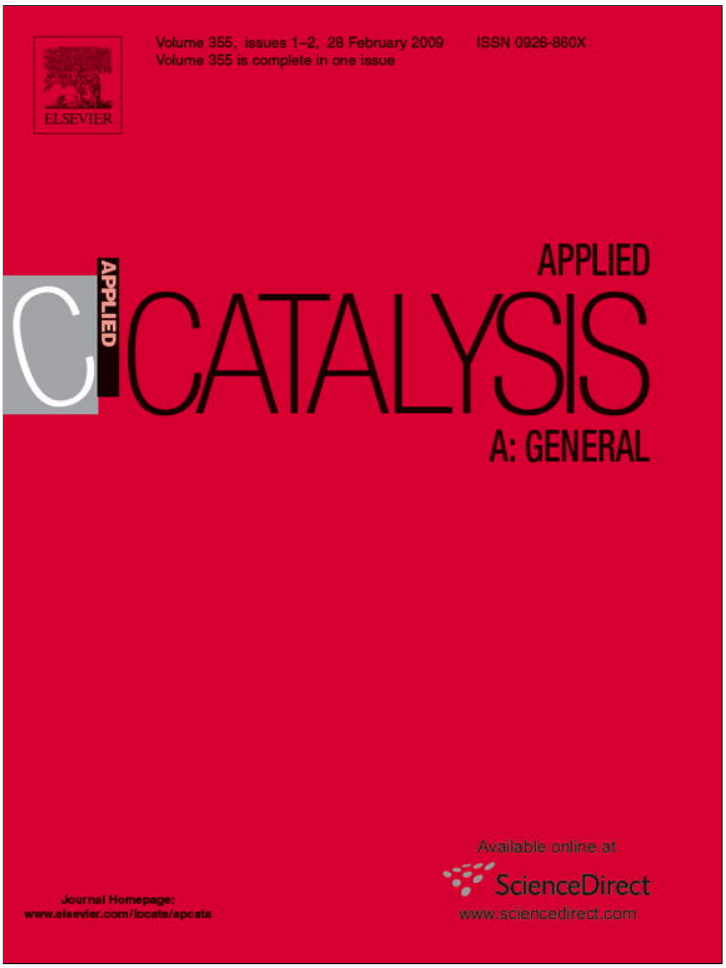

Applied Catalysis A: General 355 (2009) 50–60

Contents lists available at ScienceDirect

Applied Catalysis A: General

journal homepage: www.elsevier.com/locate/apcata

Selective hydrogenation of ethyl-benzoylacetate to 3-hydroxy-3-phenyl-propionate catalyzed by Pd/C in EtOH as a solvent in the presence of KOH: The role of the enolate ion on the reaction mechanism

L. Ronchin [a,*], A. Vavasori [a], D. Bernardi [a], G. Cavinato [b], L. Toniolo [a]

[a] Chemistry Department, Università Ca' Foscari Venezia, Dorsoduro 2137, 30123 Venice, Italy
[b] Department Chemistry Sciences, University of Padua, via Marzolo 1, 35100 Padua, Italy

ARTICLE INFO

Article history:
Received 18 August 2008
Received in revised form 3 November 2008
Accepted 18 November 2008
Available online 6 December 2008

Keywords:
Ethyl-benzoylacetate
3-Hydroxy-3-phenyl-propionate
Selective hydrogenation kinetics
Enolate adsorption

ABSTRACT

The selective hydrogenation of ethyl-benzoylacetate to 3-hydroxy-3-phenyl-propionate catalyzed by Pd/C in EtOH in a solution of KOH has been investigated. Mass transfers as well as adsorption and desorption stages do not influence reaction kinetics. A kinetic model is proposed based on the best fitting of the experimental data with Langmuir–Hinshelwood type kinetics equation. The mechanism implies that the enolate of the ethyl-benzoylacetate adsorbs strongly on two sites, thus occupying a large part of the surface Pd atoms without any reaction. The ethyl-benzoylacetate adsorbs also on two sites but with adsorption equilibrium constant almost three order of magnitude lower than that of the enolate anions. Also the hydrogen is poorly adsorbed, however, it forms Pd–H and reacts with the adsorbed keto-ester by a step hydrogenation mechanism in which the first hydride insertion is the rate-determining step. Furthermore, due to the low surface Pd–H availability and the fast desorption of the 3-hydroxy-3-phenyl-propionate the consecutive hydrogenolysis of the C–OH bond of the product is practically suppressed, thus achieving selectivity close to 100%.

1. Introduction

Partial hydrogenation of ketones to alcohols is of interest because of the hydroxyl derivatives are useful intermediate in many applications of fine chemistry [1,2]. The heterogeneously catalyzed hydrogenation of a carbonyl group is well known since the time of Sabatier [3]. It occurs with formation of a H–C–OH moiety which may undergo further hydrogenation by the C–OH bond splitting. The selectivity of different metals towards this functional group has attracted much interest [3–16].

The hydrogenation of molecules with other unsaturated sites shows further problems of selectivity. For instance, in the hydrogenation of aromatic β-keto-esters also the aromatic ring may be hydrogenated to the corresponding cyclohexyl derivative. Among the several metals active in ketones hydrogenation Pt, Pd and Rh are the most effective. The selectivity of the catalyst is related to the type of the metal and to the support [3–17]. Pd catalysts, under mild conditions, present the advantage that ring hydrogenations are completely avoided [4–7,12–15]. In addition, employing alkaline solution of ethanol in the presence of Pd/C catalysts the C–OH hydrogenolysis is practically suppressed [7,12,13] with selectivity comparable or higher than that of the Cu-based catalysts, which are highly selective but much less active [16,17]. The role of the base in the selective hydrogenation of ketones has not yet well understood, as well as that of the enolate anion, which is formed by interaction with KOH [4,5]. Kinetic studies on the hydrogenation of substituted acetophenones suggest that the enol form is not involved in the hydrogenation step, thus suggesting that keto-enol equilibrium is not a limiting step of the kinetics [8–10]. In addition, a strong dependence on the solvent polarity, typical of charged transition states, has been observed [8–10]. It has been suggested that hydrogenation occurs trough the nucleophilic attack of surface hydride species to the polarized carbonyl adsorbed on the Pd surface atoms [8,9,12,13]. In addition, it has been found that water inhibits the hydrogenolysis of the C–OH bond of ethylmandelate in EtOH catalyzed by Pd/C in the presence of HCl, due to its influence on both to the protonation equilibrium of the ester and the competitive adsorption on catalyst surface [18].

The hydrogenation of β-keto-esters is particularly studied in order to achieve high enantioselectivity in chiral compounds for pharmaceutical and fragrances industry [1,2]. The literature relating this item is large and several review and articles are available on the argument, in particular Ni, Pt and Pd supported

* Corresponding author. Fax: +39 041 2348517.
E-mail address: ronchin@unive.it (L. Ronchin).

0926-860X/$ – see front matter © 2008 Elsevier B.V. All rights reserved.
doi:10.1016/j.apcata.2008.11.028

Nomenclature

A_{ls}	interfacial area liquid/solid (m^2)
be	adsorption equilibrium constant of EBA
bk	adsorption equilibrium constant of K-EBA
bh	adsorption equilibrium constant of H_2
ce	concentration of EBA (kmol m^{-3})
ck	concentration of K-EBA (kmol m^{-3})
C	concentration (kmol m^{-3})
C_i	concentration of the reagent s at granules surface (kmol m^{-3})
D^*	effective diffusivity (m^2 s^{-1})
k	kinetic constant
k_{ls}	mass transfer coefficient of species at external liquid/solid interface (m s^{-1})
ph	partial pressure of hydrogen (kPa)
r_{H_2}	rate of hydrogen consumption (kmol m^{-3} h^{-1})
r_0	initial rate of hydrogen consumption (kmol m^{-3} h^{-1})
w	catalyst weight (kg)

Greek symbols

$\eta\phi^2$	Weeler–Weisz group
θ_X	surface coverage of the specie X
χ^2	summation of the squares of the deviations of the theoretical curve from the experimental values divided the degrees of freedom.

and unsupported metal catalysts promoted by chiral modifiers and salts are studied [19–26]. In particular, these authors studied the influences of modifiers and operative variables on reaction rates and enantiomeric excess. They observed that, together with a high enantiomeric excess obtained in the hydrogenation of prochiral ketones, in some cases the chiral modifier enhances also the catalytic activity [19,20]. In these papers, surface complex between the ketones and the modifiers are claimed and the chiral nature of the modifier is responsible for the enantioselective hydrogenation [18–26]. However, the role of the enolate ion on the reaction mechanism is not investigated and only in the old paper is mentioned [4,5].

In the present paper the kinetics of the selective hydrogenation of ethyl-benzoylacetate to 3-hydroxy-3-phenyl propionate is studied, with included the role of the enolate ion and of the water, the latter intended as an impurities present in non-negligible amount into the solvent. Several kinetic models, based on different reaction mechanism, are tested to fit the experimental data.

2. Experimental

2.1. Materials

Commercial ethyl-benzoylacetate EBA (Acros 97%) was purified by distillation under reduced pressure. Ethanol "analyzed reagent" (Baker 99%), potassium hydroxide (Carlo Erba 85%), diphenyl ether (Acros 99%), acetonitrile gradient grade (Acros), benzyl acetone (Aldrich 98%) and acetophenone (Aldrich 99%) were used without previous purification as well as the gases employed, hydrogen, nitrogen and helium research grade (purity > 99.99%, SIAD).

The catalysts Pd/C 5%: Escat 10, Escat 111 and Ru/C: Escat 40 were supplied by Engelhard Co. Pd/TiO_2 5% and Ru/TiO_2 5% were prepared by hydrolysis precipitation method described elsewhere [27].

The product of the hydrogenation of EBA, 3-hydroxy-3-phenyl-ethyl-propionate (HPEP), was separated and purified by distillation of the reaction mixture under reduced pressure.

The potassium salt of EBA (K-EBA) was prepared by reacting EBA with KOH (slight excess) in ethanol at room temperature. The precipitate that formed in a few minutes was filtered, washed with diethyl ether, dried and stored in dry box before use. NMR (in deuterate dimethyl sulfoxide Aldrich) and IR spectra showed that ester hydrolysis did not occur in detectable extent.

2.2. Equipment

Products were identified by GC, GC–MS and HPLC. GC and GC–MS analysis were carried out with a Hewlett-Packard 5890 II equipped with FID or MS detector and a OV 17 column (I.D. 250 μm 30 m long), helium was employed as carrier under the following conditions: injector 220 °C, detector 250 °C, flow 7 ml min^{-1}, oven 150 °C for 2 min 220 °C at 5 °C/min. HPLC (Hewlett-Packard HP 1050 equipped with UV detector HP1050 at λ = 205 nm) analysis were carried out in order to calculate conversion yield and selectivity at the end of reaction by a calibration with standard solution, diphenyl ether was used as internal standard. Column is a Merck C18 inverse phase at 1.5 ml min^{-1} with a solvent gradient beginning from 35% acetonitrile in water to 100% acetonitrile in 15 min. Infrared spectra have been recorded with a spectrometer Nicolet Magna IR 750. NMR spectra have been acquired with a Bruker AC 300 spectrometer. CO chemisorption has been performed with a Micromeritics ASAP 2010C automatic adsorption instrument at 308 K.

2.3. Catalyst characterization

Chemisorption of carbon monoxide was carried at 308 K with the double isotherm method and 1 min of equilibration time. The chemisorption stoichiometry was set 1 (1 molecule of CO for 1 surface Pd atom) only for comparative purpose. Before the analysis, the catalyst was pretreated with a flow of hydrogen (20 ml min^{-1}) at 473 K for 3 h and for 5 h under vacuum at the same temperature in order to ensure total reduction of the Pd particles. BET surface area of the catalysts (880 m^2 g^{-1}), average diameter of the catalyst granules (30 μm) and apparent density (540 kg m^{-3}) and void fractions (0.6) were given by the supplier and are the same for both catalysts.

2.4. Hydrogenation of EBA

Reagents and products were contained in a baffled PTFE beaker placed in a 250 ml stainless steel autoclave (AISI 316). Efficient stirring was provided by a four blades self-aspirating turbine, which allows agitation rate up to 33 Hz. Temperature control was obtained by a circulation oil thermostat (Haake mod. F3) equipped with a Pt-100 thermoresistance, which automatically allowed the control of the reactor internal temperature within 0.5 K. An auxiliary autoclave allowed the injection of the reagent into the autoclave to start the reaction at the desired pressure, which was maintained constant, within 2 kPa (between 50 and 200 kPa), by a membrane regulator and measured by a mercury manometer. The hydrogen consumption was evaluated by recording the pressure drop, detected by a piezoelectric sensor, in a vessel of known volume (5.15 or 12.72 ml) connected to the reaction autoclave by the pressure regulator (see Fig. 1). The moles of hydrogen consumed by the reaction were calculated assuming ideal behavior of the gas, since its deviation is negligible. The initial rate of reaction was calculated from pressure drop at $t \rightarrow 0$. The products

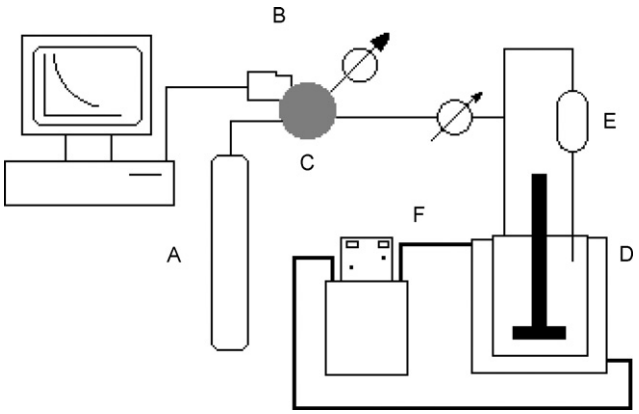

Fig. 1. Reaction equipment: (A) hydrogen reservoir, (B) PC interfaced pressure transducer, (C) pressure regulator, (D) thermostated autoclave reactor, (E) auxiliary autoclave and (F) oil circulation thermostated bath.

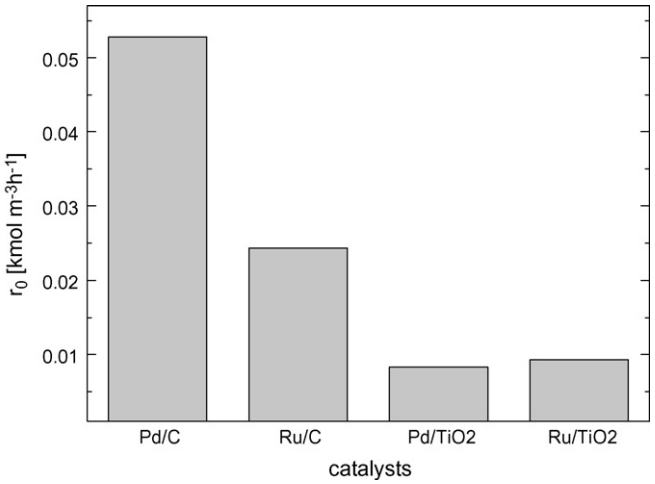

Fig. 2. Influence of the catalyst type on initial hydrogenation rate. Run conditions: catalyst 50 mg; EBA 0.1 kmol m^{-3}; KOH 10^{-4} kmol m^{-3}; reaction volume 50 ml; temperature 303 K; pressure 200 kPa.

were identified by GC, GC–MS and HPLC analysis of the liquid phase, which is periodically sampled during reaction course.

In a typical experiment 40 ml of ethanol, with suspended the Pd/C catalyst (typically 50 mg), was introduced into the reactor. After closing the reactor, it was purged with hydrogen, pressurized at 200 kPa and heated at 343 K under stirring for 2 h in order to activate the catalyst. EBA and promoters, dissolved in ethanol, were added into the auxiliary autoclave, outgased and pressurized with hydrogen at the working pressure, typically 200 kPa and injected into the reaction autoclave. After a short time (*ca.* 4 min) in order to allow temperature and pressure equilibration, stirring was started and the hydrogen consumption recorded. The first derivative at time 0 of a third order polynomial function, obtained by fitting the pressure drop *vs.* time for the first 500 s of reaction, gave the initial rate of hydrogen uptake.

2.5. Non-linear regression analysis and multivariate analysis

The methods of non-linear regression are described elsewhere and the multivariate non-linear analysis are carried out employing the built in function of the *Mathematica* package [28–30].

3. Results and discussion

3.1. Influence of operative parameters on reaction rate and selectivity

The method of initial rate changing a variable at the time has been used to study the reaction kinetics of the multiphase catalytic hydrogenation. This method has been widely used to investigate the influence of the reaction conditions on the initial rates [6,8,15,18,31]. Many authors, however, criticized kinetic model assessment by using the initial reaction rate method, suggesting more reliable results by integration of the complete concentration profile [11]. The reaction under study, however, shows a monotone reaction profile of reagents consumption and product formation without an evident formation of intermediates, thus giving poor information on the reaction pathway. As a matter of fact, only the initial rate of reaction can be consistently obtained by the concentration profile, for this reasons the model is earned by using the initial rate method and the results checked by comparing the experimental profile with that obtained by numerical integration of the model (see Fig. 15).

3.1.1. Influence of catalyst type

The results of a preliminary investigation using some Pd and Ru catalysts are reported in Fig. 2.

Despite of the differences (activity, metal, support, etc.), each catalyst gives practically 100% selectivity to the product HPEP and only traces ethyl-phenylpropanoate, from hydrogenolysis of the hydroxyl group, has been observed. Such a high selectivity is mainly due to the presence of KOH in the reaction media [7,12,13]. Pd/C catalyst is two times more active with respect to Ru/C, on the contrary Ru and Pd supported on titania show practically the same activity, which is 10 times lower than that observed with Pd/C catalysts.

Table 1 reports the effect of the Pd distribution on the reaction rate and on the turnover frequency (TOF).

TOF suggests that there is no influence of diffusion on the kinetics and that the reaction is not structure sensitive [32].

On the basis of these preliminary results, Pd/C Escat 10 catalyst has been chosen to study the influence of the operative variables on the reaction kinetics of EBA hydrogenation.

3.1.2. Influence of temperature

Arrhenius plot (Fig. 3) shows a linear trend in the range 303–333 K, the apparent activation energy of 53 kJ mol^{-1} calculated agrees to that found in literature for catalytic hydrogenations of several carbonyl compounds [7–17]. In addition, temperature has a little influence on the selectivity to HPEP, which is higher than 99% even at 333 K.

3.1.3. Influence of reagents, product and promoters

Also in this case the variation of pressure has no influence on the HPEP selectivity, which is, in any case, close to 100%. The effect of pressure on initial rate indicates an apparent reaction order of

Table 1
Influence of the Pd distribution on initial hydrogenation rate.

Catalysts Pd/C	r_0 (kmol m^{-3} h^{-1})	Pd dispersion (%)	CO adsorbed (ml g_{Pd}^{-1})	TOF (s^{-1})	Pd distribution on carbon
Escat 10	0.18	29	61.2	0.37	Uniform
Escat 111	0.13	21	44.3	0.37	Egg-shell

Run conditions: catalyst weight 50 mg; EBA 0.1 kmol m^{-3}; KOH concentration 0 kmol m^{-3}; reaction volume 50 ml; temperature 303 K; pressure 200 kPa.

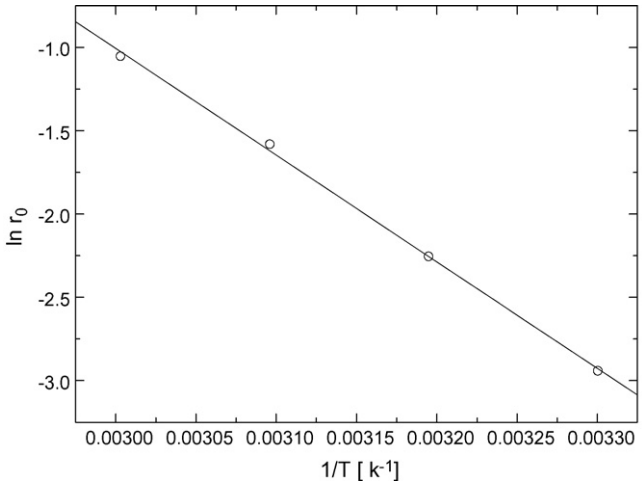

Fig. 3. Arrhenius plot for the EBA hydrogenation E_A = slope; R = 6400 8.315 = 53200 J mol^{-1}. Run conditions: catalyst 50 mg; EBA 0.1 kmol m^{-3}; KOH 10^{-4} kmol m^{-3}; reaction volume 50 ml; temperature 303–333 K; pressure 200 kPa.

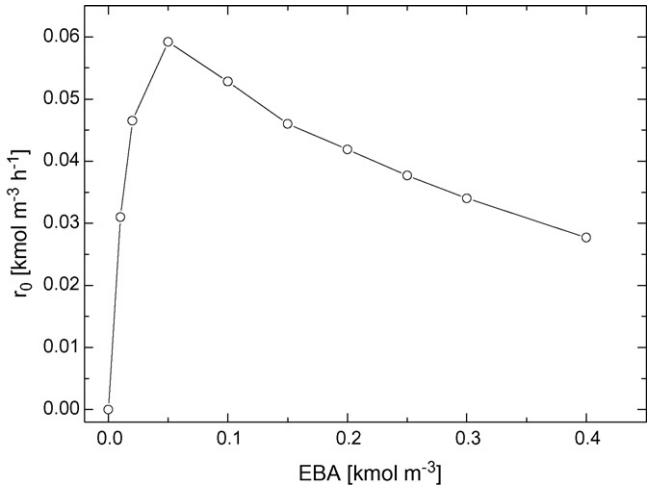

Fig. 5. Influence of EBA concentration on initial rate of hydrogenation. Run conditions: catalyst 50 mg; EBA 0–0.4 kmol m^{-3}; KOH 10^{-4} kmol m^{-3}; reaction volume 50 ml; temperature 303 K; pressure 200 kPa.

0.5 for hydrogen pressure, giving a linear plot of r_0 *vs.* $p^{0.5}$ (Fig. 4). These findings, together with what reported in literature on the hydrogen chemisorption on Pd [31,33–35], suggest that a not strongly dissociative adsorption of hydrogen on catalyst surface may occur [36]. At difference of what found in acetophenones hydrogenation, where practically an apparent zero order dependence on hydrogen pressure was found thus suggesting a strong adsorption [8]. Such a different behavior observed in EBA hydrogenation is probably related with the low availability of the sites to hydrogen, since they are prevalently occupied by other species present into the reaction mixture.

Fig. 5 shows the influence of substrate concentration on the initial rate of hydrogenation. The rate rises up to a maximum, then decreases, suggesting that upon increasing EBA concentration the catalyst sites are progressively saturated at the expenses of other active species, with a consequent lowering of the reaction rate. This trend suggests also that the rate-determining step cannot be related to the adsorption or the desorption; since in both cases a monotonic behavior should have been found. It is not clear which is the reacting species, since both enol and keto moiety could be hydrogenated to give the product and large amount of both tautomers are into the solution [37].

HPEP does not influence the reaction kinetics (Fig. 6), suggesting that desorption is fast and only a negligible part of the sites are occupied by molecules of the product.

Catalyst activity *vs.* KOH concentration is reported in Fig. 7. The trend is characterized by a fast decrease of the initial rate, up to 10 times lower of that measured in the absence of the base, followed by a stable activity at KOH concentration higher than 2×10^{-4}. It is

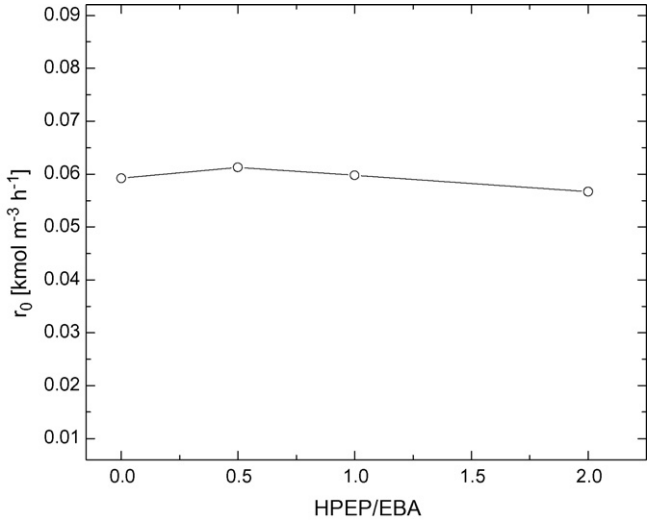

Fig. 6. Influence of the ratio product/substrate. Run conditions: catalyst 50 mg; EBA 0.05 kmol m^{-3}; KOH 10^{-4} kmol m^{-3}; reaction volume 50 ml; temperature 303 K; pressure 200 kPa.

likely that such an effect is due to the almost quantitative formation of the corresponding salt of EBA (pK_a = 10.35 [37]), which is strongly adsorbed on catalyst sites by its chelating structure. In fact, the same trend is observed by using the potassium salt of EBA (K-EBA) instead of KOH (Fig. 7), which confirms the role of the KOH on forming the enolate anion as a

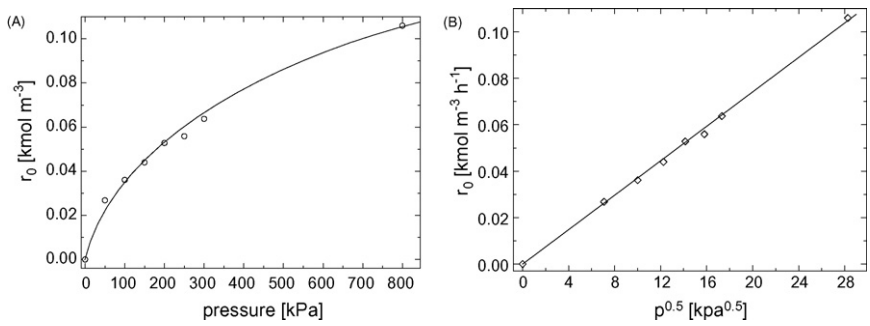

Fig. 4. Influence of hydrogen pressure on the initial rate of EBA hydrogenation. Run conditions: catalyst weight 50 mg; EBA 0.1 kmol m^{-3}; KOH 10^{-4} kmol m^{-3}; reaction volume 50 ml; temperature 303 K; pressure 0–800 kPa.

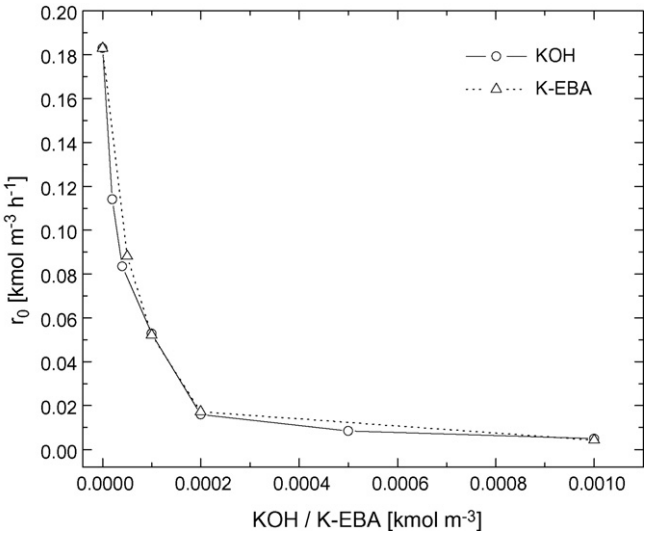

Fig. 7. Influence of KOH and K-EBA concentration on initial rate of hydrogenation. Run conditions: catalyst 50 mg; EBA 0.1 kmol m^{-3}; KOH 0–10^{-3} kmol m^{-3}; K-EBA 0–10^{-3}; reaction volume 50 ml; temperature 303 K; pressure 200 kPa.

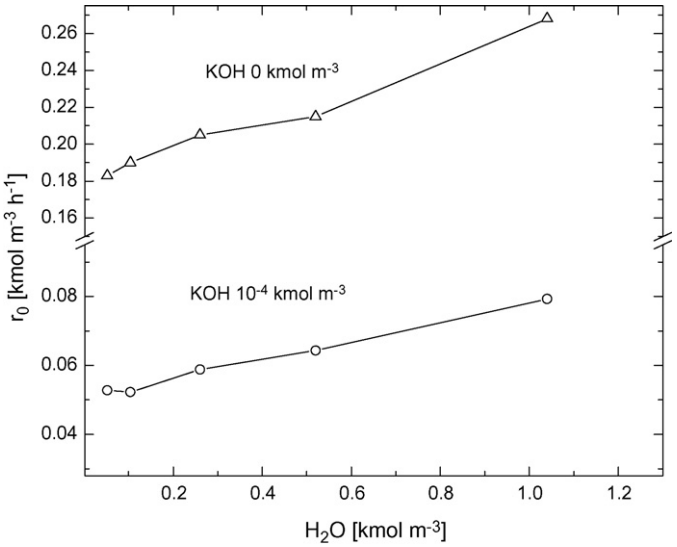

Fig. 9. Influence of H_2O concentration on initial rate of hydrogenation. Run conditions: catalyst 50 mg, EBA 0.1 kmol m^{-3}; KOH concentration 0 or 10^{-4} kmol m^{-3}; reaction volume 50 ml; temperature 303 K; pressure 200 kPa.

strongly adsorbed species. It is noteworthy that the plateau of Fig. 7 is reached when the K-EBA molecules are of the same order of magnitude of the exposed Pd atoms, thus confirming the hypothesis of strong interaction between Pd sites and the enolate anions. This is in agreement also with the poisoning effect of the nucleophiles on the hydrogenation activity of supported Pd catalysts [5]. A further confirm to this assumption, is that the hydrogenation of a suspension of K-EBA and KOH (run conditions: K-EBA 5 mmol, KOH 5 mmol solvent EtOH 50 ml, and H_2 P = 200 kPa) at 333 K in 5 h does not occur. On the light of what discussed above, the enhancement of the selectivity is probably due to both, the low availability of surface hydride, and the fast desorption of the product. Such a hypothesis is in agreement with the kinetic data reported in literature relevant to the hydrogenation of ketones, alcohol and nitro compounds [5,8,18,38]. In all cases a zero apparent reaction order for hydrogen was found, suggesting that strong hydrogen adsorption occurs on catalyst surface [5,8,18,38]. On the contrary, we found an apparent reaction order for hydrogen of 0.5 suggesting dissociative chemisorption for hydrogen and low surface occupation (Fig. 4) [36].

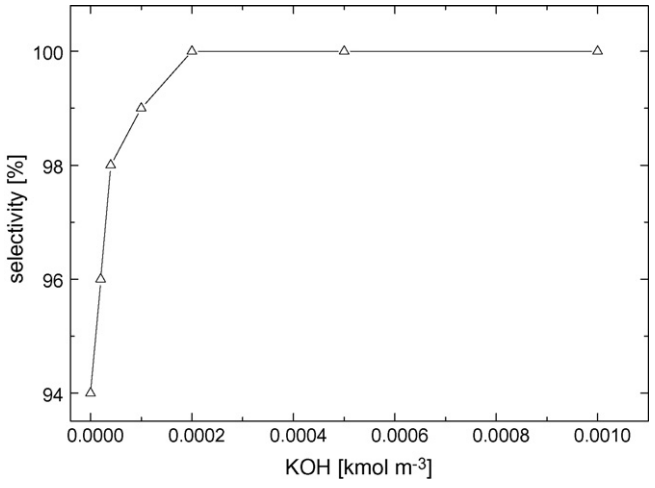

Fig. 8. Influence of KOH concentration on conversion and selectivity after 2 h. Run conditions: catalyst 50 mg; EBA 0.1 kmol m^{-3}; KOH 0–10^{-3} kmol m^{-3}; reaction volume 50 ml; temperature 303 K; pressure 200 kPa.

In Fig. 8 selectivities after 2 h of reaction are reported. The trend is analogous to that observed for the initial rate with a steep increasing of the selectivity reaching practically 100% at KOH concentration of 2×10^{-4} kmol m^{-3}.

Figs. 9 and 10 show the influence of water on initial reaction rate and on the selectivity of the reaction. The reaction rate slightly increases as the concentration of water rises independently of the presence of KOH, whereas selectivity decreases both in the presence and in the absence of KOH. These evidences suggest that the role of water cannot be ascribed to a change of the enolate equilibria, since the effect of water is practically the same with or without base. The increase of reaction rate may be ascribed to a change of solvation of the reacting species, rather than a direct involvement of the water on reaction mechanism. Such a hypothesis is in agreement with what found for acetophenones hydrogenation where a linear relationship with the variation of the dielectric constant of the solvent has been observed [8].

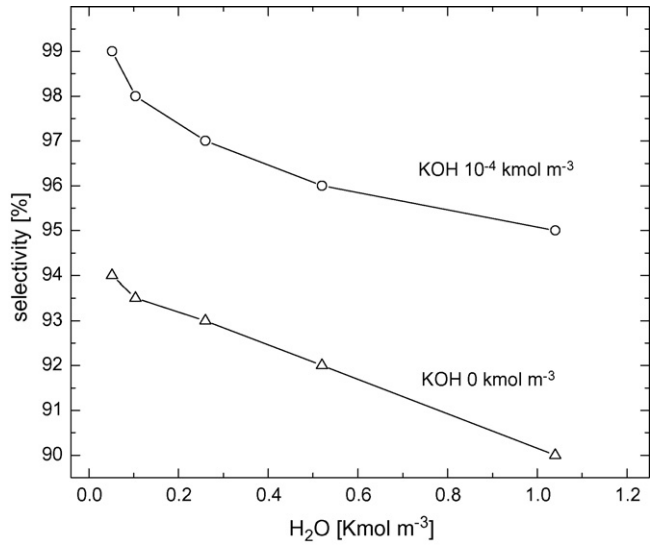

Fig. 10. Influence of H_2O concentration on selectivity after 2 h. Run conditions: catalyst 50 mg, EBA 0.1 kmol m^{-3}; KOH concentration 0 or 10^{-4} kmol m^{-3}; reaction volume 50 ml; temperature 303 K; pressure 200 kPa.

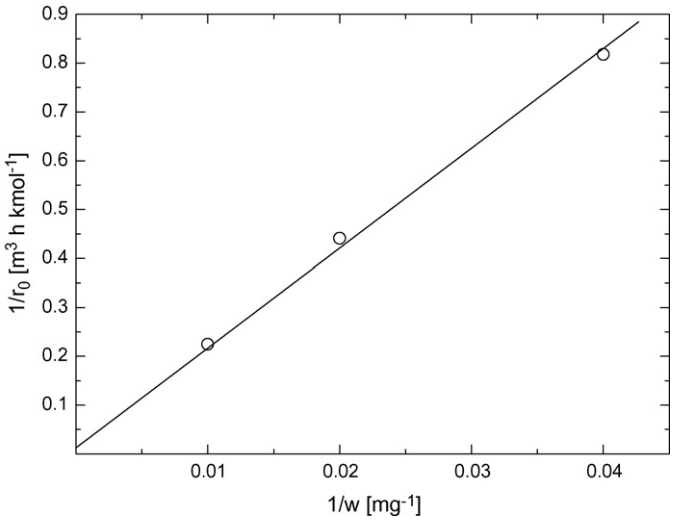

Fig. 11. Influence of catalyst amount on the initial rate of EBA hydrogenation. Run conditions: catalyst 25–100 mg; EBA 0.1 kmol m^{-3}; KOH 10^{-4} kmol m^{-3}; reaction volume 50 ml; temperature 303 K; pressure 0–300 kPa.

3.2. Some thought on the kinetics of reaction

3.2.1. Determination of kinetic regime

The kinetics of multiphase gas/liquid/solid reactions may be limited by diffusive phenomena at the interfaces or into the pores of the catalysts [38,39]. The gas/liquid mass transfer does not affect the reaction rate, since varying the agitation speed between 13 and 25 Hz and the catalyst loading the overall rate does not change significantly. This is confirmed also by the, the reciprocal values of the intercept of the plot $1/r$ *vs.* $1/w$ (Fig. 11), which is almost 20 times higher than the highest measured rate [38,39]. In order to check if mass transfer at liquid/solid interface is the limiting step, the observed reaction rates are compared with the diffusive mass transfer rate calculated considering that instantaneous reaction occurs in the pores [38,39]. In the case of liquid solid mass transfer control the rate of hydrogen consumption the kinetics would be given by the following equation:

$$-r_{H_2} = K_{ls} A_{ls} (C - C_i) \quad (1)$$

where k_{ls} (m s^{-1}) is the mass transfer coefficient at liquid/solid interface of each reagent, A_{ls} (m^2) the liquid/solid interface area, the concentration of the reagent C_i (kmol m^{-3}) at the catalyst surface and C (kmol m^{-3}) is the concentration of the reagent in solution. The values of k_{ls} for hydrogen and ethyl-benzoylacetate are 7.4×10^{-4} and 1.6×10^{-4} m s^{-1}, respectively estimated by the reported correlation [38,39]. The values of A_{ls} ($A_{ls} = 1.8 \times 10^{-2}$ m^2) is calculated by following Eq. (2) in the approximation of spherical particles:

$$A_{ls} = \frac{6w}{d_g \rho_g} \quad (2)$$

where w (kg) is the catalyst amount, d_g (m) the average diameter of the catalyst granules and ρ_g (kg m^{-3}) is the density of the granules filled with the solution [38]. Concentration of hydrogen at the operating conditions (pressure: 200 kPa, temperature: 333 K) is about 7 mol m^{-3} and the concentration of the ester is 100 mol m^{-3} [38]. Then the limiting diffusion rates, calculated by taking into account that surface concentration (C_i) approach to zero when a fast reactions occurs into the granule, are for hydrogen and EBA are 5.7×10^{-5} and 1.8×10^{-4} mol s^{-1}, respectively [38,39]. The comparison of the previous results with the higher measured hydrogen consumption rate (2.55×10^{-6} mol s^{-1} at 333 K) allows to state that the observed rates are not limited by liquid/solid diffusion.

The influence of intraparticles diffusion on reaction kinetics can be checked by calculating the values of Wheeler–Weisz number for the reagents by the following equation:

$$\eta\Phi^2 = \frac{(-r_{H_2} d_p^2)}{(4D * V_c C)} \quad (3)$$

where d_p (m) is the mean particles diameter, D^* (m^2 s^{-1}) is the effective diffusivity calculated taking into account tortuosity factor and the void fractions, V_c (m^3) is the catalyst volume [38,39]. The values of $\eta\Phi^2$ calculated for hydrogen and EBA are respectively 0.41 and 0.15 suggesting that the diffusion of the reagent into the pores of the catalyst is not the limiting step of the reaction kinetics [38,39]. This is experimentally confirmed by an apparent activation energy of 56 kJ mol^{-1}, which is much higher than that of diffusive phenomena [38]. Moreover, the comparison of catalysts with the same average diameter of the granule, but with different metal distribution into the granule itself, shows constant values of the TOF (Table 1).

3.2.2. Kinetic models

In Section 3.1 the influence of the operative variables on the reaction kinetics have been investigated by analyzing the initial rate of hydrogenation. In this section we discus only the most reliable models, which have been selected for both physical and/or mathematical reasons (see Appendix A). The widely used Langmuir–Hinshelwood kinetic equations are in many cases lacking of physical meaning due to the complexity of the surface equilibria [40]. Sometimes, these models are not only able to fit experimental data but also have a suitable physical meaning, specially when high coverage of the surface is achieved and the reactions are not structure sensitive [40]. In this case, both conditions are satisfied, then, we consider in our models the following starting point: (1) all the catalyst sites are equivalent, (2) Pd metal dissociates H_2 giving Pd–H species, (3) both EBA and K-EBA can bind 1 or 2 surface Pd atom. On the basis of these assumptions four reaction pathways (Scheme 1) are possible. A relationship between the geometry of carbonyl adsorption and the number of sites involved in the process is beyond the scope of the work. Even though, it seems to be only a speculative matter since under the actual reaction conditions fast interconversion between the parallel and the end-on configuration may probably occur, due to the low energy difference between the two state (the end-on is 19 kJ mol^{-1} more stable) [41]. The reactions of Scheme 1, by applying the generally accepted Horiuty-Polanyi step hydrogenation mechanism by two consecutive surface hydride insertion [5,8], give eight different simultaneous equations (see Appendix A) taking into account that the rate-determining step can be one of the two consecutive surface reaction. Because of the negligible influence of the product on the reaction rate the rate-determining step can be considered irreversible. The choice of the first hydride insertion as the rate-determining step seems to be more likely than the second one in agreement with what reported in literature on ketones and aldehydes hydrogenation [31,34,42–46]. Furthermore, on considering the second hydride insertion as the limiting step, only monotonic rate equations *vs.* ester concentration are obtained (see Appendix A). In this way, by taking into account what have been discussed in Section 3.1 it is possible to state:

(i) hydrogen has an apparent reaction order of 0.5 in agreement with dissociative adsorption and low hydrogen coverage on Pd surface (Fig. 4) [36];
(ii) the maximum in the initial rate of reaction *vs.* EBA concentration suggests that adsorption and desorption are not the limiting step of the kinetics (Fig. 5);

Mechanism LH11

$H_2 + 2s$	⇌	2H-s	1
EBA + s	⇌	EBA-s	2
K-EBA + s	⇌	K-EBA-s	3
EBA-S + H-s	⇌	EBAH-s + s	4
EBAH-s + H-s	⇌	HPEP-s	5
HPEP-s	⇌	HPEP + s	6

Mechanism LH21

$H_2 + 2s$	⇌	2H-s	1
EBA + 2s	⇌	EBA-s	2
K-EBA + s	⇌	K-EBA-s	3
EBA-s + H-s	⇌	EBAH-s + s	4
EBAH-s + H-s	⇌	HPEP-s	5
HPEP-s	⇌	HPEP + s	6

Mechanism LH12

$H_2 + 2s$	⇌	2H-s	1
EBA + s	⇌	EBA-s	2
K-EBA + 2s	⇌	K-EBA-s	3
EBA-S + H-s	⇌	EBAH-s + s	4
EBAH-s + H-s	⇌	HPEP-s	5
HPEP-s	⇌	HPEP + s	6

Mechanism LH22

$H_2 + 2s$	⇌	2H-s	1
EBA + 2s	⇌	EBA-s	2
K-EBA + 2s	⇌	K-EBA-s	3
EBA-s + H-s	⇌	EBAH-s + s	4
EBAH-s + H-s	⇌	HPEP-s	5
HPEP-s	⇌	HPEP + s	6

Scheme 1. Reactions pathways.

Table 2
Kinetic equations obtained from pathways of scheme 1.

Model	Equation	Adsorption: coverage and stoichiometry
LH11	$wk\frac{be\cdot ce\cdot\sqrt{bh\cdot ph}}{(1+be\cdot ce+bk\cdot ck)^2}$	Small coverage of H_2; 1 site for EBA; 1 site for K-EBA.
LH12	$wk\frac{be\cdot ce(\sqrt{(1+be\cdot ce)^2+8bk\cdot ck}-be\cdot ce-1)\sqrt{\frac{bh\cdot ph((1+be\cdot ce)^2+4bk\cdot ck-(\sqrt{(1+be\cdot ce)^2+8bk\cdot ck}\cdot(1+be\cdot ce)))}{bk^2ck^2}}}{bk\cdot ck\sqrt{128}}$	Small coverage of H_2; 1 site for EBA; 2 site for K-EBA.
LH21	$wk\frac{be\cdot ce\left(\frac{bh\cdot ph\cdot\left(4be\cdot ce-(bk\cdot ck+1)\cdot\left(\sqrt{8be\cdot ce+(1+bk\cdot ck^2)}-1-bk\cdot ck\right)\right)}{be^2ce^2}\right)^{3/2}}{\sqrt{512}bh\cdot ph}$	Small coverage of H_2; 2 site for EBA; 1 site for K-EBA.
LH22	$wk\frac{be\cdot ce\left(\frac{bh\cdot ph\cdot\left(1+4be\cdot ce+bk\cdot ck+\sqrt{1+8be\cdot ce+8bk\cdot ck}\right)}{(be\cdot ce+bk\cdot ck)^2}\right)^{3/2}}{\sqrt{512}bh\cdot ph}$	Small coverage of H_2; 2 site for EBA; 2 site for K-EBA.

(iii) KOH reacts quantitatively with EBA to K-EBA, which adsorbs strongly on catalyst;
(iv) the product does not influence the kinetics suggesting irreversible surface reactions, low product coverage and fast desorption (Fig. 6);
(v) first hydride insertion is supposed to be the rate-determining step.

Starting from the above considerations, by applying the stationary state hypothesis to the adsorption equilibria and considering the first hydride insertion as the irreversible rate-determining step, four sets of simultaneous equations are obtained (see Appendix A). Their solutions give a large ensemble of algebraic expressions, but only those reported in Table 2 (one for each model) have physical meaning (Fig. 12).

The large number of constants involved in the models does not allow to obtain a reliable estimate of the whole set of parameters simply by fitting the experimental data since highly correlation between the parameters has been observed that gives poor

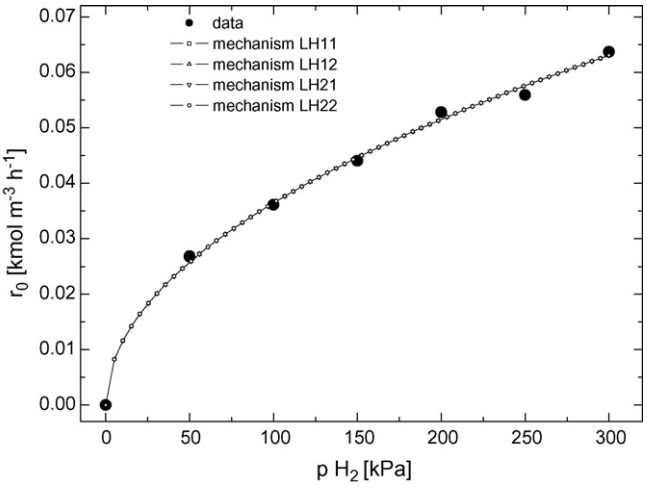

Fig. 12. Fittings results: influence of hydrogen pressure on initial reaction rate.

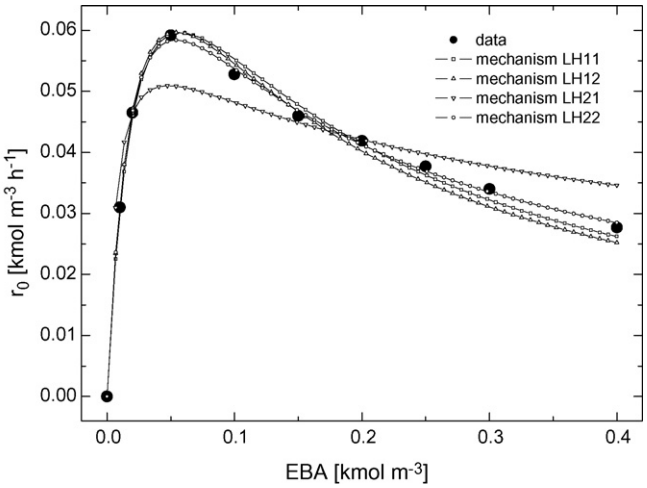

Fig. 13. Fittings results: influence of EBA concentration on initial reaction rate.

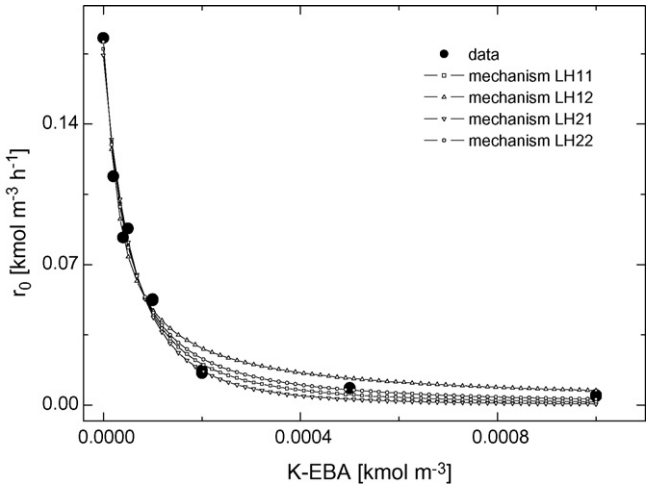

Fig. 14. Fittings results: influence of K-EBA concentration on initial reaction rate.

Table 3
Fittings results of the models derived from the mechanisms of Scheme 1.

Mechanism	*wk*	*be*	*bk*	χ^2
Influence of H_2 pressure on reaction rate				
LH11	1.64	11.46	1,228	1.6E−6
LH12	1.61	12.10	1,227	1.7E−6
LH21	3.27	12.10	1,225	1.6E−6
LH22	1.47	30.19	7,730	1.6E−6
Influence of EBA concentration on reaction rate				
LH11	3.50	36.1	10,746	2.7E−6
LH12	1.86	20.2	1,001	4.6E−6
LH21	3.50	30.7	2,151	2.0E−5
LH22	0.57	5.97	3,524	6.0E−7
Influence of K-EBA concentration on reaction rate				
LH11	5.04	8.87	18,367	5.0E−5
LH12	7.33	4.58	26,930	9.0E−5
LH21	10.01	5.88	12,139	9.0E−5
LH22	0.59	5.01	4,595	4.0E−5

significance of these values. As a matter of fact infinite set of estimator can be found with poor statistical meaning [29,47]. For this reason, in order to validate the models it is necessary to verify if reliable parameters can fit experimental data. As a matter of fact, we set $bh = 10^{-4}$ (H_2 constant of adsorption), an arbitrary value compatible with the hypothesis of the models (negligible adsorption of H_2 compared with both EBA and K-EBA). Then, *be*, *bk*, and *k* are estimated by fitting experimental data minimizing χ^2 function (summation of the squares of the deviations of the theoretical curve from the experimental values divided the degrees of freedom). In Table 3 and in Figs. 13–15 are reported the results of the stepwise fittings of the kinetic equations applied to a singular effect data set. This preliminary analysis allows to directly discard the model LH21 since does not satisfactorily fit experimental data (Fig. 14). At this stage, the numerical values of the parameters obtained by stepwise fitting are meaningless but the comparison between the constant of adsorption of K-EBA and EBA (ratio $bk/be > 10^2$ to 10^3) suggests the adsorption of K-EBA is 2–3 orders of magnitude stronger than EBA, confirming the poisoning effect of the enolate anions [5,12].

A better discrimination of the models is the multivariate fitting because of convergence for inconsistent models is more difficult [29]. Reliable starting parameters have been obtained from the stepwise analysis and in Table 4 are reported the results of the fittings. As expected, LH21 does not reach convergence according to the poor results obtained in the stepwise fitting, thus giving a further evidence of the lack of the model. The others reach convergence but both LH11 and LH12 don not hold, since the errors are larger than the values of the parameters. Only LH22 model hold because the errors are compatible with the values of the parameters. The clearest result on the goodness of the LH22 model can be observed in Fig. 15, where only the LH22 model gives values in agreement to the experimental data. Furthermore, only for the LH22 model the residuals are distributed around zero and these do not show any trend with various parameters [29,47].

The simulation of the conversion profile by numerical integration of the kinetic equation of LH22 model is in agreement the

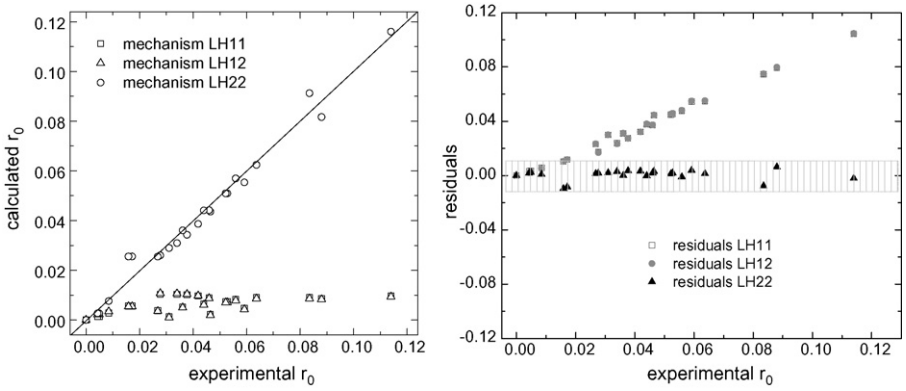

Fig. 15. Multivariate fitting results: comparison of the models.

Table 4
Multivariate fitting analysis of the models derived from mechanisms of Scheme 1.

Mechanism	*wk*	Error	*be*	Error	*bk*	Error	χ^2
LH11	2.90	9.29	44.3	196	34,600	14,668	9.2E−4
LH12	3.08	8.29	57.2	194	63,600	43,244	5.4E−4
LH21	–	–	–	–	–	–	–
LH22	0.366	0.085	3.80	0.768	2,491	504	1.5E−5

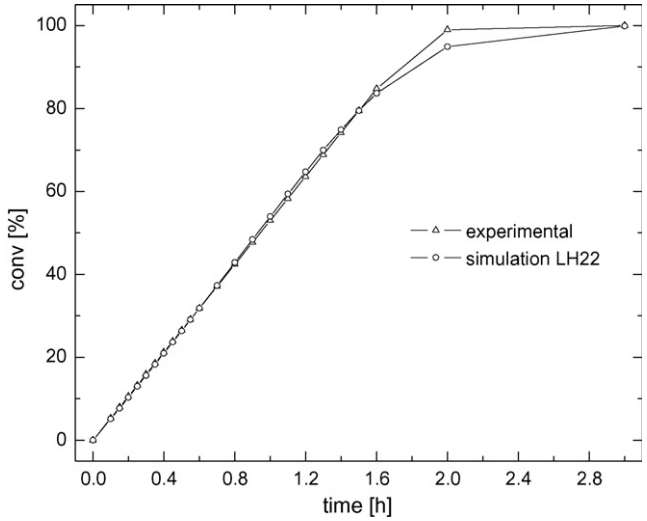

Fig. 16. Comparison of simulated and experimental conversion. Run conditions: catalyst 50 mg; EBA 0.1 kmol m^{-3}; KOH 10^{-4} kmol m^{-3}; reaction volume 50 ml; temperature 303 K; pressure 200 kPa. Experimental conversion obtained from hydrogen consumption.

experimental trend (Fig. 16), giving a further evidence of the goodness of the model.

The above kinetic analysis, however, does not give quantitative kinetic or thermodynamic data, for this reason the values of both equilibrium and kinetic constants must be considered as simple indication of a likely mechanism on the base of the experimental evidences. Quantitative data on adsorption equilibrium of the species are beyond the scope of the present work.

4. Conclusions

The kinetics of hydrogenation of ethyl-benzoylacetate in EtOH–KOH solution has been studied giving new insights on the mechanism of β-keto-esters hydrogenation. KOH reacts quantitatively with EBA giving the enolate salt K-EBA which has a poisoning effect on the catalytic surface. Under this condition, the selectivity to 3-hydroxy-3-phenyl propionate is almost 100%. Such a behavior is mainly due to the following reasons:

(a) strong adsorption of K-EBA, which diminish the availability of surface hydride;
(b) hydrogen is poorly adsorbed and dissociative adsorption occurs;
(c) the adsorbed enolate ions is not reactive;
(d) the product is poorly adsorbed fast desorbed.

The kinetic model agrees with adsorption of EBA and K-EBA on two sites (see Scheme 2) and the rate-determining step is the first hydride insertion. Moreover, the deactivating effect of the enolate anion accords to the large value of the adsorption constant of K-EBA with respect to that of the EBA. Differently of what expected from previous results of ethylmandelate hydrogenolysis, water depresses selectivity increasing both overall rate and HPEP hydrogenolysis.

Acknowledgements

Ca' Foscari University of Venice is gratefully acknowledged for financial support (Ateneo fund 2006) and the Engelhard Company of Milan for generous loan of catalysts.

Appendix A

Here we explain the choice of the kinetic equations employed on the fitting. Langmuir–Hinshelwood type kinetic equations, in view of simple bimolecular irreversible surface reactions, have the general form $r = wk\theta_X\theta_Y$ where $\boldsymbol{\theta}_X$ and $\boldsymbol{\theta}_Y$ are the coverage of the reacting species. Starting from this assumption, a large number of Langmuir–Hinshelwood models can be obtained then for practical reasons, only those which have both physical and mathematical significance have been employed on fitting the experimental data (e.g. all the parameters are fixed positive). Furthermore, it is widely accepted that hydrogen is dissociatively adsorbed on Pd catalysts during hydrogenation reactions [31,44–46], therefore we rule out *a priori* the models based on the nondissociative hydrogen chemisorption.

Langmuir–Hinshelwood models with specific sites of adsorption for different species give 32 simultaneous equations by considering all the possible mechanism involving one or two sites for each reagent and the possibility of two or three specific sites of adsorption are obtained. The resulting functions of each models has been studied in order to verify its physical or mathematical relevance on fitting the data. All these models are discarded since the mathematical functions cannot fit experimental data. For instance, in many cases only monotonic rate equation *vs.* ester concentration is obtained, while the experimental observations show a trend with a maximum (for more detail see additional materials). For the same reason in Section 3.1.3, we ruled out adsorption and desorption stages as rate-determining step.

In Table A1 are reported the equations obtained by considering the equivalence of the catalyst sites in the adsorption of the reagents, thus considering one irreversible surface reaction as the rate-determining step (the first or the second hydride insertion see Scheme 1), we obtain 8 set of simultaneous equations.

The hypothesis that hydrogen is poorly adsorbed allows to neglect $\boldsymbol{\theta}_H$ from the surface mass balance thus giving a great simplification in the calculations [31]. In the first part of Table A1 are reported the equations relating the mechanisms in which the first hydride insertion is the rate-determining step (LH11, LH12, LH21, and LH22 models). The study of these functions shows that the trends are compatible with those of the experimental observations. On the contrary, when second hydride insertion is considered as the rate-

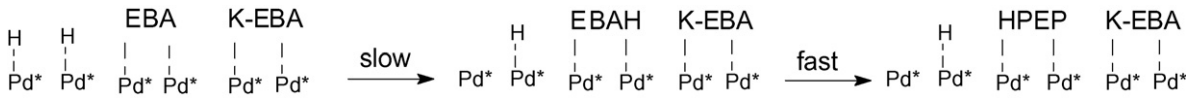

Scheme 2. Surface reaction mechanism.

Table A1
Simultaneous equations derived by equivalent site of adsorption from the model of Scheme 1.

Equations obtained on considering as the rate-determining step the irreversible first hydride reaction with the carbonyl			
$bh = \frac{\theta_H^2}{ph \cdot \theta_F^2}$	LH11 consistent with data	$bh = \frac{\theta_H^2}{ph \cdot \theta_F^2}$	LH21 consistent with data
$be = \frac{\theta_E}{ce \cdot \theta_F}$		$be = \frac{\theta_E}{ce \cdot \theta_F^2}$	
$bk = \frac{\theta_K}{ce \cdot \theta_F}$		$bk = \frac{\theta_K}{ce \cdot \theta_F}$	
$r = wk \cdot \theta_E \cdot \theta_H$		$r = wk \cdot \theta_E \cdot \theta_H$	
$1 = \theta_E + \theta_K + \theta_F + \theta_H$		$1 = \theta_E + \theta_K + \theta_F + \theta_H$	
$1 \cong \theta_E + \theta_K + \theta_F$		$1 \cong \theta_E + \theta_K + \theta_F$	
$bh = \frac{\theta_H^2}{ph \cdot \theta_F^2}$	LH12 consistent with data	$bh = \frac{\theta_H^2}{ph \cdot \theta_F^2}$	LH22 consistent with data
$be = \frac{\theta_E}{ce \cdot \theta_F}$		$be = \frac{\theta_E}{ce \cdot \theta_F^2}$	
$bk = \frac{\theta_K}{ce \cdot \theta_F^2}$		$bk = \frac{\theta_K}{ce \cdot \theta_F^2}$	
$r = wk \cdot \theta_E \cdot \theta_H$		$r = wk \cdot \theta_E \cdot \theta_H$	
$1 = \theta_E + \theta_K + \theta_F + \theta_H$		$1 = \theta_E + \theta_K + \theta_F + \theta_H$	
$1 \cong \theta_E + \theta_K + \theta_F$		$1 \cong \theta_E + \theta_K + \theta_F$	
Equations obtained on considering as the rate-determining step the irreversible second hydride reaction with the hemi-hydrogenated-carbonyl			
$bh = \frac{\theta_H^2}{ph \cdot \theta_F^2}$	SLH11 monotone with reagents concentration not consistent with data	$bh = \frac{\theta_H^2}{ph \cdot \theta_F^2}$	SLH21 monotone with reagents concentration not consistent with data
$be = \frac{\theta_E}{ce \cdot \theta_F}$		$be = \frac{\theta_E}{ce \cdot \theta_F^2}$	
$bk = \frac{\theta_K}{ce \cdot \theta_F}$		$bk = \frac{\theta_K}{ce \cdot \theta_F}$	
$K = \frac{\theta_S \cdot \theta_F}{\theta_E \cdot \theta_H}$		$K = \frac{\theta_S \cdot \theta_F}{\theta_E \cdot \theta_H}$	
$r = wk \cdot \theta_S \cdot \theta_H$		$r = wk \cdot \theta_S \cdot \theta_H$	
$1 = \theta_E + \theta_K + \theta_F + \theta_S + \theta_H$		$1 = \theta_E + \theta_K + \theta_F + \theta_S + \theta_H$	
$1 \cong \theta_E + \theta_K + \theta_F + \theta_S$		$1 \cong \theta_E + \theta_K + \theta_F + \theta_S$	
$bh = \frac{\theta_H^2}{ph \cdot \theta_F^2}$	SLH12 monotone with reagents concentration not consistent with data	$bh = \frac{\theta_H^2}{ph \cdot \theta_F^2}$	SLH22 monotone with reagents concentration not consistent with data
$be = \frac{\theta_E}{ce \cdot \theta_F}$		$be = \frac{\theta_E}{ce \cdot \theta_F^2}$	
$bk = \frac{\theta_K}{ce \cdot \theta_F^2}$		$bk = \frac{\theta_K}{ce \cdot \theta_F^2}$	
$K = \frac{\theta_S \cdot \theta_F}{\theta_E \cdot \theta_H}$		$K = \frac{\theta_S \cdot \theta_F}{\theta_E \cdot \theta_H}$	
$r = wk \cdot \theta_S \cdot \theta_H$		$r = wk \cdot \theta_S \cdot \theta_H$	
$1 = \theta_E + \theta_K + \theta_F + \theta_S + \theta_H$		$1 = \theta_E + \theta_K + \theta_F + \theta_S + \theta_H$	
$1 \cong \theta_E + \theta_K + \theta_F + \theta_S$		$1 \cong \theta_E + \theta_K + \theta_F + \theta_S$	

determining step (SLH11, SLH12, SLH21, and SLH22 models), the functions appear to be unsuitable to fit experimental data. For this reasons the SLH11, SLH12, SLH21, and SLH22 models are discarded.

The non-linear nature of the equations give multiple solutions for each set of simultaneous equations, however only the expressions, whose parameters have values in the range of significance, are reported in Table 2 and employed on fitting the data.

Appendix B. Supplementary data

Supplementary data associated with this article can be found, in the online version, at doi:10.1016/j.apcata.2008.11.028.

References

[1] W.F. Ringk, in: Kirk Othmer (Ed.), Enciclopaedia of Chemical Technology, vol. 6, John Wiley & Sons, 1980, p. 142.
[2] D. Anderson, G. Frater, US Pat. 6,348,618 B1 (2002).
[3] P. Sabbatier, J.B. Senderens, Compt. Rend. 137 (1904) 301.
[4] R.L. Augustine, Catal. Today 37 (1997) 419.
[5] R. Baltzly, J. Org. Chem. 41 (1976) 920.
[6] E. Rocchini, R. Spogliarich, M. Graziani, J. Mol. Catal. 91 (1994) 313.
[7] P.N. Rylander, Hydrogenation Methods, Academic Press, 1985.
[8] M.A. Aramendia, V. Borau, J.F. Gomez, J. Catal. 140 (1993) 335.
[9] H. Van Bekkum, A.P.G. Kieboom, K.J.G. Van de Putte, Rec. Trav. Chim. 88 (1969) 52.
[10] M. Bonnet, P. Geneste, Y. Lonzano, C.R. Acad. Sci. Paris Ser. C 282 (1976) 1009.
[11] M.V. Rajashekharam, R.V. Chaudhari, Chem. Eng. Sci. 51 (1996) 1663.
[12] P.N. Rylander, Catalysis in Organic Synthesis, Academic Press, 1978 155.
[13] E. Breitner, E. Roginski, P.N. Rylander, J. Org. Chem. 24 (1959P) 1855.
[14] R.V. Malyala, C.V. Rode, M. Arai, S.G. Hegde, R.V. Chaudari, Appl. Catal. A: Gen. 193 (2000) 71.
[15] P. Maki-Arvela, S. Sahin, N. Kumar, T. Heikkila, V. Lehto, T. Salmi, D.Y. Murzin, Appl. Catal. A: Gen. 350 (2008) 24.
[16] F. Zaccheria, N. Ravasio, R.A. Psaro, Fusia Tetrahedron Lett. 46 (2005) 3695.
[17] N.M. Bertero, C.R. Apesteguia, A.J. Marchi, Appl. Catal. A: Gen. 349 (2008) 100.
[18] L. Ronchin, L. Toniolo, G. Cavinato, Appl. Catal. A: Gen. 165 (1997) 133.
[19] S. Diezi, S. Reimann, N. Bonalumi, T. Mallat, A. Baiker, J. Catal. 239 (2006) 255.
[20] U.K. Singh, M.A. Vannice, Appl. Catal. A: Gen. 213 (2001) 1.
[21] T. Osawa, Y. Hagino, T. Harada, O. Takayasu, Catal. Lett. 112 (2006) 57.
[22] T. Osawa, Y. Amayaa, T. Harada, O. Takayasu, J. Mol. Catal. A 211 (2004) 93.
[23] E.I. Klabunovskii, Kinet. Catal. 33 (1992) 233.
[24] G. Szollosi, B. Herman, K. Felfoldi, F. Fulopa, M. Bartok, J. Mol. Catal. A 290 (2008) 54.
[25] I. Bucsi, M. Sutyinszki, K. Felfoldi, M. Bartok, Catal. Commun. 7 (2006) 104.
[26] S. Nakagawa, A. Tai, T. Okuyama, T. Sugimura, Top. Catal. 13 (2000) 187.
[27] L. Ronchin, L. Toniolo, React. Kinet. Catal. Lett. 78 (2003) 281.

[28] L. Ronchin, L. Toniolo, Appl. Catal. A: Gen. 208 (2001) 77.
[29] D.M. Bates, D.G. Watts, Non-linear Regression Analysis & its Applications, John Wiley & Sons, New York, 1988.
[30] M.L. Abell, J.P. Braselton, The Mathematica Handbook, Academic Press, 1992.
[31] N. Chang, S. Aldrett, M.T. Holtzapple, R.R. Davison, Chem. Eng. Sci 55 (2000) 5721.
[32] C.N. Satterfield, Heterogeneous Catalysis in Industrial Practice, II ed., McGraw-Hill, 1991.
[33] P.H.T. Philipsen, E.J. Baerends, J. Phys. Chem. B 110 (2006) 12470.
[34] V. Pallassana, M. Neurock, J. Phys. Chem. B 104 (2000) 9449.
[35] J. Roques, C. Lacaze-Dufaure, C. Mijoule, J. Chem. Theory Comput. 3 (2007) 878.
[36] J.B. But, Reaction Kinetics and Reactor Design, 2nd ed., Marcel-Dekker, NY, 2000, pp. 169.
[37] S. Singer, P. Zuman, J. Org. Chem. 39 (1974) 836.
[38] G.W. Roberts, in: P.N. Rylander, H. Greenfield (Eds.), Catalysis in Organic Synthesis, Academic Press, 1976, p. 1.
[39] P.A. Ramachadran e, R.V. Chaudhari, Three-phase Catalytic Reactors, Gordon and Breach Sciences Publisher, 1982.
[40] M. Boudart, Ind. Eng. Chem. Fundam. 28 (1986) 656.
[41] E.L. Jeffery, R.K. Mann, G.J. Hutchings, S.H. Taylor, J.W. David, Catal. Today 105 (2005) 85.
[42] A. Van Der Burg, J. Doornbos, N.J. Kos, W.J. Ultee, V. Ponec, J. Catal. 54 (1978) 243.
[43] G.M.R. van Druten, L. Aksu, V. Ponec, Appl. Catal. A: Gen. 149 (1997) 181.
[44] G.M.R. Van Druten, V. Ponec, Appl. Catal. A: Gen. 191 (2000) 153.
[45] G.M.R. Van Druten, V. Ponec, Appl. Catal. A: Gen. 191 (2000) 163.
[46] H.U. Blaser, H.P. Jalett, M. Garland, M. Studer, H. Thies, A. -Tijani, J. Catal. 173 (1998) 282.
[47] N.R. Draper, H. Smith, Applied Regression Analysis, John Wiley & Sons, New York, 1966, pp. 86.